

Chemical and Structural Characterization of Zirconium Nitride Produced by External Gelation and Neutronic Performances

Osama Farid, Nader Mohamed

Reactor Department, Atomic Energy Authority, Cairo, Egypt

Email address

usamafa98@hotmail.co.uk (O. Farid)

Citation

Osama Farid, Nader Mohamed. Chemical and Structural Characterization of Zirconium Nitride Produced by External Gelation and Neutronic Performances. *American Journal of Chemistry and Application*. Vol. 6, No. 2, 2019, pp. 12-17.

Received: March 27, 2019; Accepted: May 19, 2019; Published: May 30, 2019

Abstract: Materials used in fuel elements in next generation of nuclear power are expected to be more efficient than previous materials and are also expected to be subject to harsher thermal and radiation environments. Zirconium nitride (ZrN) exhibits exceptional mechanical, chemical, and electrical properties for use as component for Gas-cooled Fast Reactor (GFR) fuel. This work improved current understanding of processing and thermophysical properties of zirconium nitride, also neutronic performance of (U-Pu)N fuels. A newly developed external gelation produced zirconiumoxynitride pellets, and their structure and growth was characterized by SEM and XRD. XRD analysis of the ZrN showed the samples had formed highly crystalline solid solutions during sintering. The resulting thermal conductivity of ZrN_x and Zr-biphasic material would still meet the melting temperature requirements of GFR fuel materials of 2200 K. The differences in the properties observed were due to the different gelation mechanisms involved and the physical form of the matrix produced. The neutronic performance of the (U-Pu)O₂ and (U-Pu)N fuels (80 wt.% natural uranium and 20 wt.% plutonium reactor grade) has been studied using Monte Carlo N-Particle Transport Code System (MCNPX 2.7.0 code). Due to the higher density of heavy metals in (U-Pu)N fuel than in (U-Pu)O₂ fuel, (U-Pu)N, this fuel achieved longer irradiation times.

Keywords: Gas-Cooled Fast Reactor, Non-oxide Ceramics, Zirconium Nitride Fabrication, Nuclear Fuels Microstructure, MCNPX 2.7.0 Code

1. Introduction

Supporting energy demands for an increasing population has led to a renewed interest worldwide in nuclear power. The Gas-cooled Fast Reactor (GFR) is one of the reactor concepts selected by the Generation IV International Forum (GIF) for the next generation of innovative nuclear energy systems. The design goal for this fast reactor is to combine various features, including high coolant temperature and flexible breeding parameters [1]. The high coolant temperature allows for both high thermodynamic efficiency and the possibility for heat applications, e.g. hydrogen production. Non-oxide ceramics such as the carbides and nitrides of group IV transition metal elements have an interesting mixture of ionic, covalent and metallic bonding. This combination of bonding gives the materials an unusual mixture of advantageous properties such as high hardness (25 GPa) and very high melting temperatures (3000K) along with good thermal and electrical conductivity

(10 Wm⁻¹K⁻¹ and 200×10⁴m⁻¹ respectively) [2, 3]. As a result of these properties the carbide and nitride of uranium or plutonium are receiving increased attention for use in advanced nuclear power plants (NPP) [4, 5].

Current fuel concepts are designed as fissile material diluted in a non-fissile material which has a low neutron capture cross section. This concept offers increased safety by reducing the maximum fuel temperature that would be reached by having pure fissile material in the core, whilst producing no further transuranic waste material [6].

Several fuel design concepts (plates, rod pins and pebbles) are being investigated and various codes are being developed and/or adapted to improve the quality of the results, and also to reduce the computing time required for the burnup/depletion simulation of these heterogeneous fuel designs; all working in a fast neutron energy spectrum [7, 8]. Neutron transparent oxide and non-oxide matrices are listed in table 1.

Table 1. Current designed candidate as fissile material diluted in a non-fissile matrix.

Matrix Type	Fissile material	Non-fissile matrix
Oxide	ThO ₂ , UO ₂	BeO, MgO, Y ₂ O ₃ , ZrO ₂ , CeO ₂
Binary oxide	ThO ₂ , UO ₂	MgAl ₂ O ₄ , Y ₃ Al ₅ O ₁₂ , ZrSiO ₄
Oxide solid solution	(U, Th)O ₂ , (Pu, U)O ₂	Mg _(1-x) Al _(2+x) O _(4-x)
Carbide	ThC ₂ , ThC, UC, PuC	SiC, TiC, ZrC
Nitride	ThN, UN, PuN	AlN, TiN, ZrN, CeN

Historically, the fuel burnups have gradually increased with time. Light Water Reactors (LWRs) fueled with UO₂ are licensed of fuel enrichment up to 5%w U²³⁵ and burnup up to 60 MWd/kg. However, there is a trend to increase the fuel burnup up to 100 MWd/kg which needs around 8%w U²³⁵ enrichment. This would depend on the development progress in the fuel and fuel cladding fabrication. A thorough knowledge of how the structure and bonding of the materials gives rise to the high hardness, melting temperature and Thermophysical properties will be advantageous in their processing and production and for predicting their evolution during the fuels lifetime [9, 10]. However, the fuel of the reactors should be highly enriched, fast reactors are breeders of fissile isotopes which make the fuel reactivity decreases very slowly with the irradiation time enabling very long irradiation time of the fuel. In this case, Simulation of GFR lattice cell using MCNPX 2.7.0 code for the (U-Pu)O₂ and (U-Pu)N fuels is extremely important. This simulation will help understanding the maximum fuel burnup that the fuel can withstand harsh environment [11]. Zirconium nitride is being considered for use as an inert matrix fuel or as advanced fuel particle coatings due to its high thermal conductivity, low neutron capture cross section and chemical compatibility with existing fuel cycle technology. The aim of this work is to enhance understanding of ionotropic external gelation technique and carbothermic reduction-nitridation to produce ZrN ceramics as fuel components in advanced nuclear fuels, also to investigate the Thermophysical properties. Using MCNPX 2.7.0 code is to contribute to knowledge of thermal conductivity, neutron capture cross section, and chemical compatibility with existing fuel cycle technology.

2. Experimental

Microspheres containing ZrN were prepared by the ionotropic external gelation technique using Zr²⁺. This technique involves interaction of a cation (or an anion) with an ionic polymer to generate a highly cross linked structure. External gelation is the preferred method in producing cross-linked alginate for coating due to the different gelation mechanisms involved and the physical form of the matrix produced. Powders of ZrO₂ and C (Sigma Aldrich) were mixed in a ratio to achieve a C/Zr molar ratio of 2.7 and 3.0. These mixtures were homogenized by ball milling for 12 h and dried at 363 K. Powders were heated at 2073 K for 4 h in a furnace to produce the corresponding carbides by carbothermic reduction. The resulting powders were then ball milled for 12 h and dried. Nitridation of dried powders was carried out for 8–10 h at 1800–2100 K under a flowing atmosphere of 10% H₂–90% N₂ gas in a tube furnace. Sintering was carried out for 1 h at 2273 K (+10 K/min). Ranges of powder sizes and grain sizes in the ceramics were measured by SEM. Density is calculated as the mean of four measurements using the Archimedes method. Phase analysis was performed by X-ray diffraction (XRD) using 40 kV and 40 mA, using Ni-filtered CuK α radiation. Surface microstructure was characterized by SEM and chemical analysis performed used EDX. Grain boundaries were revealed by thermal etching, (heating to 1400°C for 2 hours in vacuum, <0.001ppb O₂) and chemical etching (with a mixture of 1:1:1 HF:HNO₃:H₂O). Sintering conditions along with density and grain boundary analysis are shown in table 2.

Table 2. Sintering parameters and sample density.

Sample	temp / °C	time/ min	Pressure / MPa	Density / g cm ⁻³	% theoretical density	Mean grain size / μ m
ZrN-1	1800	8	50	6.36	83.6	^a
ZrN-2	1900	10	60	6.70	90.0	^a
ZrN-3	2100	10	50	6.88	93.5	^a
ZrN-4	2100	10	50	7.09	99.0	29-38

^aNot determined

The results evaluated during the production of dense ZrN samples, with time, temperature and piston pressure. The optimization of the sintering process only led to >99% dense ZrN as this is the upper limit of achievable temperature and operational piston pressure.

3. Results and Discussion

3.1. Thermophysical Properties of ZrN

The optimization of the sintering process lead to study

sample no ZrN-4. SEM image and EDX of ZrN showing are shown in figure 1. Thermal diffusivity was measured using laser flash and thermal conductivity was calculated from these measurements using equation 1,

$$k = \alpha \rho C_p \quad (1)$$

where α is the thermal diffusivity (m²/s), ρ is the density (Kg m⁻³) and C_p is the heat capacity (J Kg⁻¹ K⁻¹). Heat capacity was calculated using equation 2,

$$C_p^\circ = A + (BT) + C*T^2 + D*T^3 + E/T^2 \quad (2) \quad \text{where } C_p \text{ is heat capacity and } T \text{ is temperature (K)/1000, \text{ along with constants } A, B, C, D \text{ and } E.$$

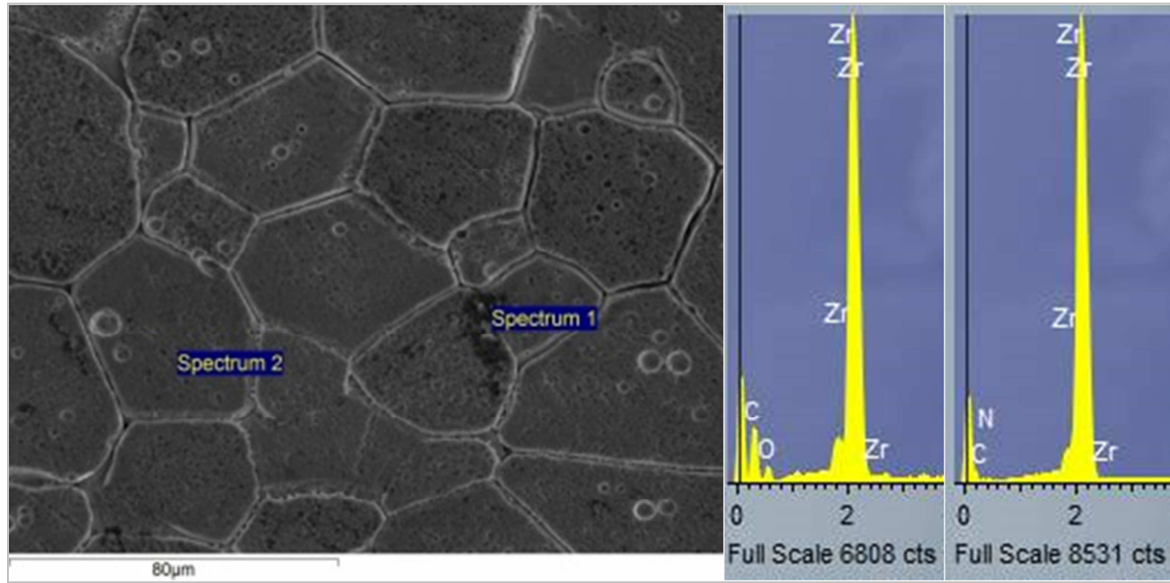


Figure 1. SEM image of ZrN showing dark phase a) EDX spectrum 1 b) EDX spectrum 2.

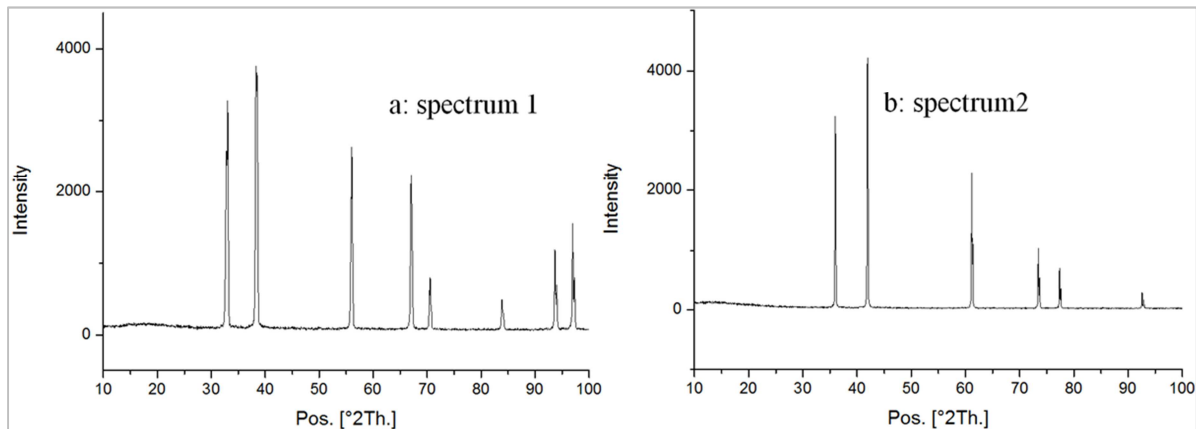
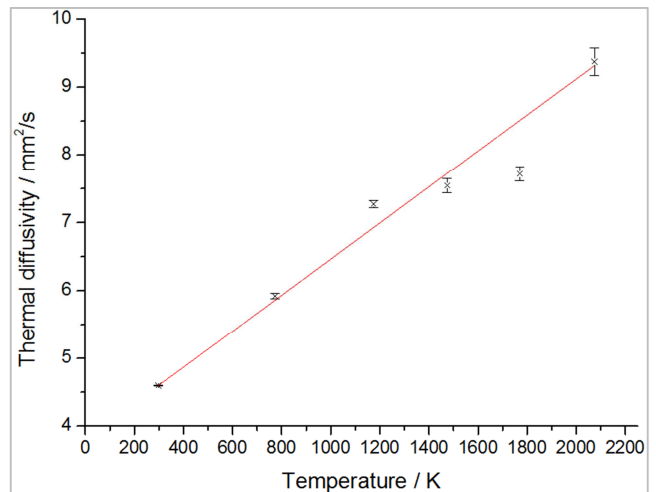


Figure 2. XRD of two samples ZrN.

EDX revealed the phases at the grain boundary consisted of Zr, C and O, although XRD in figure 2 indicated a single phase of ZrN. The presence of oxygen may be due to the thermal etching, however the treatment was carried out at 10^{-6} Torr with <0.001 ppb O_2 , carbon may be present due to residue or diffusion from the graphite die used. Thermal etching induced grain growth as the average grain size is larger than reported [4]. EDX analysis again showed the presence of zirconium, carbon and oxygen in these dark regions. Oxide impurities may also be present from the starting powder as the powder is $\geq 99\%$. Quantification of these contaminants is not possible by EDX as it is semi-quantitative analysis. XRD in figure 2 showed single phase monoliths were present in both spectrums. XRD revealed Zr, N system existed as one FCC phase except for a small amount (<1 wt%) of oxide phases present, supporting the co-existence of the two phases. A single phase ceramic is not a strict requirement but control of the microstructure becomes more important if the composite exists as two phases, density of these two phases will also be

important as higher densities will give structural stability and increase thermal conductivity.



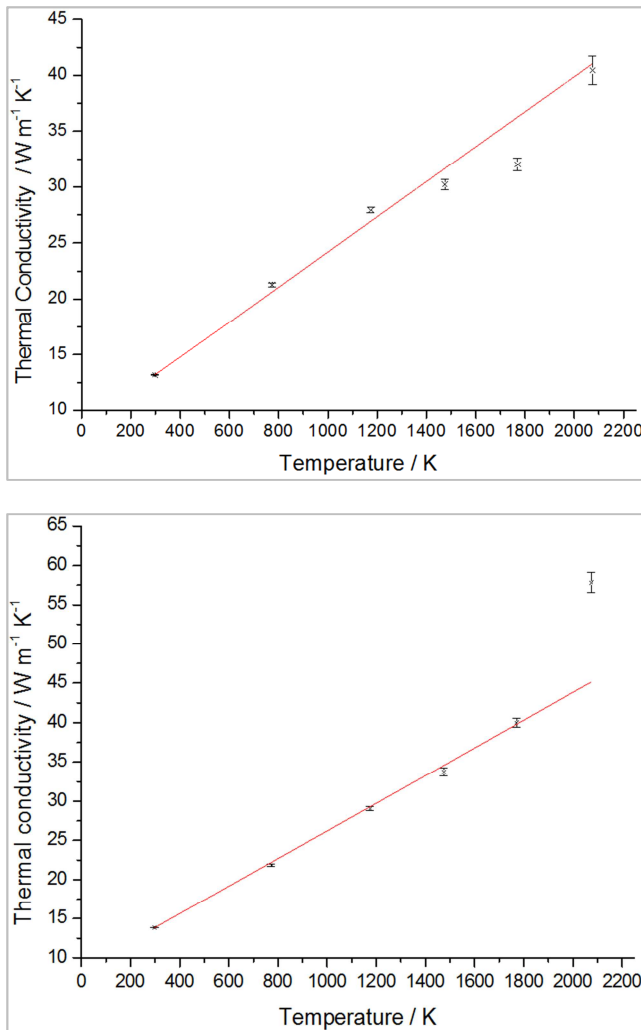


Figure 3. a) Thermal diffusivity against temperature, b) thermal conductivity against temperature using heat capacity values, c) Thermal conductivity of ZrN sample using heat capacity values.

It can be seen from figure 3 that the thermal diffusivity and therefore the thermal conductivity both increase with increasing temperatures with values of thermal conductivity in the region of 20–40 $\text{W m}^{-1} \text{K}^{-1}$ in the range of temperatures that the material was exposed. Results showed the thermal diffusivity measurements obtained between 25 - 1800°C along with preliminary thermal conductivity data calculated using reported heat capacity values [12, 13].

3.2. Neutronic Performance

The neutronic performances have been studied using the Monte Carlo code MCNPX2.7.0 [14]. The code is compatible with MCNP5 with many additional capabilities including material depletion/burnup calculations. All standard evaluated nuclear data libraries used by MCNP can be used by MCNPX 2.7.0. Data libraries containing particle-interaction can be replaced by physics models if the libraries are not available. The program also includes cross-section measurements, benchmark experiments, deterministic code development, and improvements in transmutation code and library tools through the CINDER90 project. The neutron cross section data for the

fuel, the moderator and cladding were recalled from ENDF/B-VII.0. The data of fuel was recalled at a temperature of 900 K [15].

The gas-cooled fast reactor core design is still under development. Different designs for the fuel have been developed. Rod geometry has been selected in this study [16]. The fuel assembly is built from 271 fuel rods arranged in a hexagonal mesh as shown in figure 4. The fuel is clad by zirconium nitride with a gap helium between the fuel and its clad. Lattice cell calculations have been carried out for (U-Pu) O_2 and (U-Pu)N fuels such that 80 wt.% of the heavy metals is natural uranium and 20 wt.% is plutonium reactor grade.

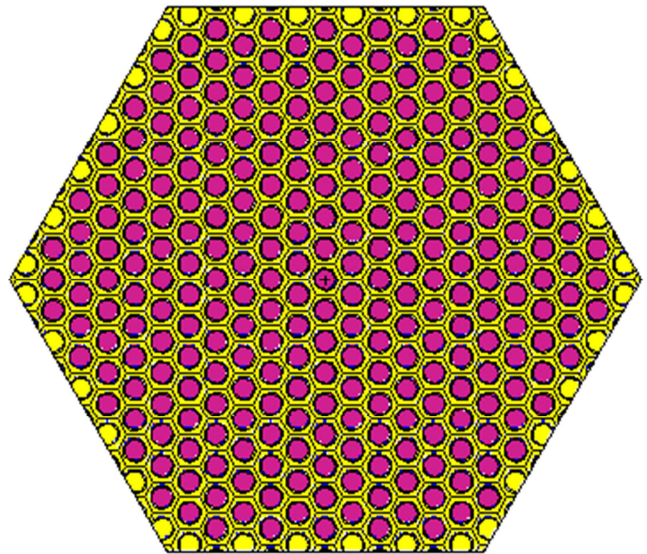


Figure 4. GFR lattice cell as simulated using MCNP.

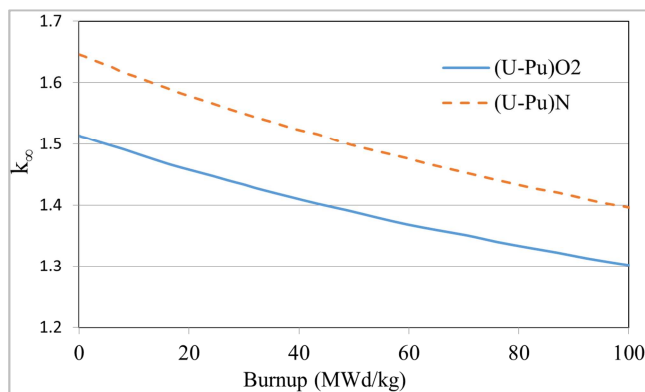
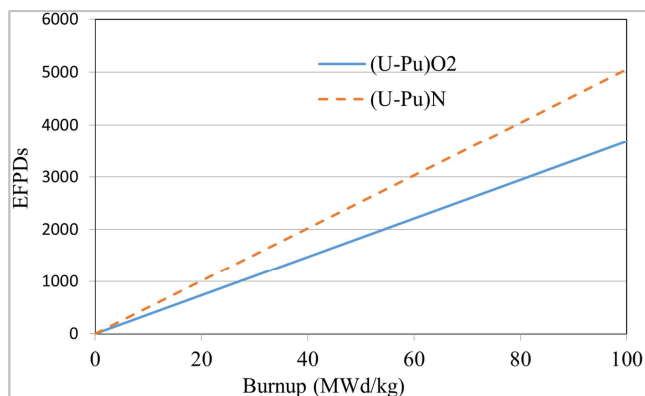
It is assumed that the plutonium is produced after 52 MWd/kg U burnup of 4.5% w. U-235 UO_2 in a pressurized water reactor. The plutonium isotope distribution is 2.8% w. Pu-238, 50.3% w. Pu-239, 24.1% w. Pu-240, 11.6% w. Pu-241 and 3.6% w. Pu-242. Table 3 gives the compositions of the (U-Pu) O_2 and (U-Pu)N fuels used in this study. Other data used in the simulation is presented in Table 4 [17]. The depletion histories (k_{∞}) against the burnup for (U-Pu) O_2 and (U-Pu)N fuels are shown in Figure 5. The calculations are carried out until the fuel was burnt to 100 MWd/kg. Figure 6 gives the Effective Full Power Days (EFPDs) as function of the burnup of the two fuel types.

Table 3. Fuel data used in simulation.

Fuel Type	(U-Pu) O_2	(U-Pu)N
Nitrogen enrichment	-	99.6%w. N-15
Density (95% theoretical, g/cm^3)	10.55	13.585
Uranium isotopic Distributions (%w.)	U-238	99.28
	U-235	0.72
	Pu-238	2.8
Plutonium isotopic Distributions (%w.)	Pu-239	50.3
	Pu-240	24.1
	Pu-241	11.6
	Pu-242	3.6

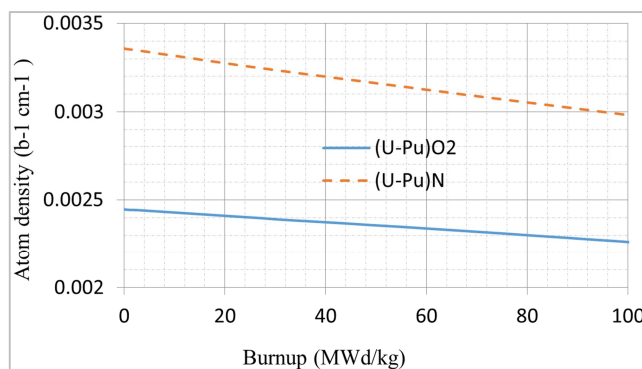
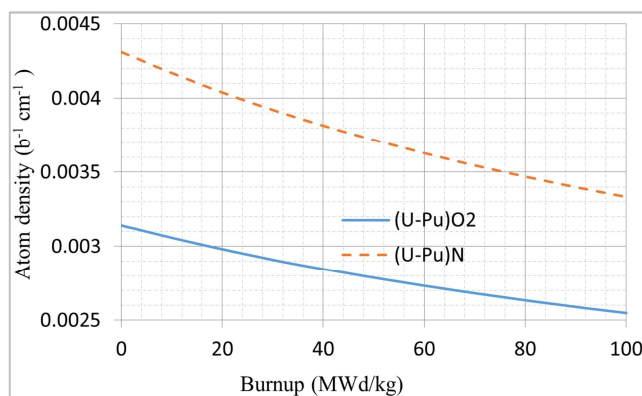
Table 4. Lattice cell data used in simulation.

Parameter	Data
Reactor power density (W/cm ³)	100
Assembly geometry	Hexagonal
Assembly pitch (cm)	11.16
Number of rods per assembly	271
Rod cell geometry	Hexagonal
Rod cell pitch (cm)	0.64
Rod diameter (cm)	0.85
Gap thickness (cm)	0.003
Gladding material	Zirconium nitride
Gladding density (g/cm ³)	6.55
cladding thickness (cm)	0.05

Figure 5. Depletion histories for (U-Pu)O₂ and (U-Pu)N fuels.Figure 6. EFPDs as function of the burupnup of (U-Pu)O₂ and (U-Pu)N fuels.

In GFR, the fuel would be discharged at the end of core cycle after from 60 to 100 MWd/kg with high reactivity as shown in Figure 6. Therefore, the dry processing would extract 60 MWd/kg or more from the recycled fuel which make the process economically attractive. As mentioned above, the irradiated fuel is treated in thermal-mechanical processing plant where the fuel cladding is replaced, the fission gasses are captured and the fuel is re-fabricated. This in turn makes the fuel withstand a new irradiation cycle in the reactor. The dry processing plant would be built in the site of the GFR to minimize the cost of transportation. The recycling of the irradiated fuel would be until the irradiated fuel has insufficient reactivity for a new cycle. Due to the higher density of heavy metals in (U-Pu)N fuel than in (U-Pu)O₂ fuel, (U-Pu)N fuel achieves longer irradiation times than in case of (U-Pu)O₂ fuel.

Variations of the atomic densities with the burnup of Pu-239 and the sum of the main fissile isotopes (Pu-239, Pu-241 and U-235) are given in Figures 7 and 8, respectively for the (U-Pu)O₂ and (U-Pu)N fuels.

Figure 7. Variations of the atomic densities of Pu-239 with the burnup of (U-Pu)O₂ and (U-Pu)N fuels.Figure 8. Variations of the atomic densities of the main fissile isotopes (U-235, Pu-239 and Pu-242) with the burnup of (U-Pu)O₂ and (U-Pu)N fuels.

Due to the higher density of the (U-Pu)N fuel, its burnup rate is smaller than that in the case of (U-Pu)O₂ fuel as shown in Figure 7. After a burnup of 100 MWd/kg, the atomic density of Pu-239 decreases by 7.8% and 11.5% in the (U-Pu)O₂ and (U-Pu)N fuels, respectively as shown in Figure 8. 100 MWd/kg achieves 3670 EFPDs for the (U-Pu)O₂ fuel and 5010 EFPDs for the (U-Pu)N. this means that the decrease rate of Pu-239 is slightly higher in the (U-Pu)N fuel than in the (U-Pu)O₂ fuel. However, the total of the fissile isotopes decrease by 19.3% and 23.2% for the (U-Pu)O₂ and (U-Pu)N fuels, respectively and therefore the decrease rate of the total fissile isotopes is slightly lower in the (U-Pu)N fuel than in the (U-Pu)O₂ fuel.

4. Conclusion

The processing route and fabrication of ZrN from ZrO₂ using ionotropic external gelation technique using Zr²⁺ has been studied with the focus largely on the nitridation step of ZrN_x compositions. The product was analyzed immediately by XRD to avoid any room temperature oxidation. Nitridation experiments was performed in ammonia atmosphere which has greater activity of nitridation process. The rate of

nitridation was increased with increasing times and temperatures of the nitridation reaction. However, even after long reaction times (24 h) all samples still contained carbon impurities and preliminary analysis of nitridation progress as a function of time indicates a reduction in rate with reaction time although a more comprehensive study of rate kinetics study is needed.

Simulation of GFR lattice cell using MCNPX 2.7.0 code for the (U-Pu)O₂ and (U-Pu)N fuels, with 80% w. of the HM is natural uranium and 20% w. reactor grade plutonium, showed that the (U-Pu)N fuel is higher reactive and would achieve longer irradiation times (longer EFPDs). The irradiation time would be controlled by the licensing burnup. Dry processing is a potential solution for direct recycling of the GFR spent fuel which would reduce the fabrication costs. Fast reactors are breeders of fissile isotopes which make the fuel reactivity decreases very slowly with the irradiation time enabling very long irradiation time of the fuel.

References

- [1] J. C. Hedge, J. W. Kopec, C. Kostenko, J. L. Lang, Thermal Properties of Refractory Alloys, US Air Force Report, ASD-TDR 63-597, 1963.
- [2] N. Chauvin, R. J. M. Konings, H. Matzke, Optimization of Inert Matrix Fuel Concepts for Americium Transmutation, Journal of Nuclear Materials, (1999), 274, 105-111.
- [3] P. C. Stevenson and W. E. Nervik, The Radiochemistry of the Rare Earths, Scandium, Yttrium, and Actinium, National Academy of Sciences National Research Council Nuclear Series, NAS-NS 3020, February 1961.
- [4] Y. Arai, K. Nakajima, Preparation and Characterization of PuN Pellets Containing ZrN and TiN, Journal of Nuclear Materials, 281, 244-247, 2000.
- [5] M. Salvatores, G. Palmiotti, Radioactive Waste Partitioning and Transmutation Within Advanced Fuel Cycles: Achievements and Challenges, Progress in Particle and Nuclear Physics, (2011), 66, 144-166.
- [6] Y. Arai, K. Minato, Fabrication and Electrochemical Behavior of Nitride Fuel for Future Applications, Journal of Nuclear Materials, 344, 180-185, 2005.
- [7] V. Basini, J. P. Ottaviani, J. C. Richaud, M. Streit, F. Ingold, Experimental Assessment of Thermophysical Properties of (Pu, Zr)N, Journal of Nuclear Materials, 344, 186-190, 2005.
- [8] A. Ciriello, V. V. Rondinella, D. Staicu, J. Somers, Thermophysical Characterization of Nitrides Inert Matrices: Preliminary Results on Zirconium Nitride, Journal of Nuclear Materials, 371, 129-133, 2007.
- [9] J. L. Collins, M. F. Lloyd, and R. L. Fellows, The Basic Chemistry Involved in the Internal-Gelation Method of Precipitating Uranium as Determined by pH Measurements, Radiochim. Acta, (1987), 42, 121-34.
- [10] T. Nakagawa, H. Matsuoka, M. Sawa, M. Hirota, M. Miyake, M. Katsura, Formation of Uranium and Cerium Nitrides by the Reaction of Carbides with NH₃ and N₂/H₂ Stream, Journal of Nuclear Materials, 247, 127-130, 1997.
- [11] Matthew Bunn, Steve Fetter, John P. Holdren, Bob Van Der Zwaan, "The Economics of Reprocessing Vs. Direct Disposal of Spent Nuclear Fuel," Final Report 8/12/1999-7/30/2003, President and Fellows of Harvard University, 2003.
- [12] M. W. Chase, Jr., NIST-JANAF (National Institute of Standards and Technology, Thermochemical Tables, Fourth Edition, J. Phys. Chem. Ref. Data, Monograph 9, (1998), 1-1951.
- [13] J. Adachi, K. Kurosaki, M. Uno, S. Yamanaka, Thermal and Electrical Properties of Zirconium Nitride, Journal of Alloys and Compounds, (2005), 399, 242-244.
- [14] Pelowitz, D. B., 2011. MCNPX User's Manual, Version 2.7.0. Los Alamos National Laboratory.
- [15] P. Petkevich, K. Mikityuk, P. Coddington, S. Pelloni, R. Chawla, Comparative Transient Analysis of a Gas-cooled Fast Reactor for Different Fuel Types, Proceedings of ICAPP '06, Reno, NV USA, June 4-8, 2006.
- [16] Nader M. A. Mohamed, Alya Badawi, "Effect of DUPIC Cycle on CANDU Reactor Safety Parameters" Nuclear Engineering and Technology, 48 (5), 2016.
- [17] Ricardo Reyes-Ramírez, Cecilia Martín-del-Campo, Juan-Luis François, Emeric Brun, Eric Dumonteil, Fausto Malvagi, "Comparison of MCNPX-C90 and TRIPOLI-4-D for fuel depletion calculations of a Gas-cooled Fast Reactor," Annals of Nuclear Energy 37 (2010) 1101-1106.